Primary Radicals Production from Water Fragmentation by Heavy Ions

E. C. Montenegro
Instituto de Física, Universidade Federal do Rio de Janeiro,
Cx. Postal 68528, Rio de Janeiro, RJ 21941-972, Brazil

and H. Luna
School of Physical Sciences, Dublin City University, Glasnevin D9, Dublin, Ireland

Received on 3 December, 2004

The importance of fragmentation of water molecules by heavy ions is discussed for several different physical environments, including tumor treatment, planetary sciences and fission reactors. The characteristics of the fragmentation yields by electrons, protons and photons are presented and compared with fragmentation yields of water molecules by C^{3+} and O^{5+} ions at energies corresponding to the Bragg peak. It is shown that for low energy electron loss and high energy electron capture, the water molecules essentially blow-out, releasing a much larger fraction of O^{q+} ions as compared with electrons, protons and photons.

I. INTRODUCTION

Water is the main component of our bodies, covers most of Earth surface, is found in several moons of our planetary system and has been continuously brought to our vicinities by comets, revealing part the distant history of our solar system formation. In all these scenarios the water molecules can be found bombarded by photons as well as by a variety of particles coming from several different sources: the Sun, planetary magnetospheres, radioactive sources, particle accelerators or nuclear power plants, for example. These ionizing radiations have the power to transform the benefic water molecule in quite reactive pieces. When water molecules are splitted due to the action of these particles, very reactive fragments are produced which strongly interfere on the nearby environment. Different particles produce different fragmentation yields which must be known to model the complex chain of reactions which follow the primary products.

The splitting of water by photons is a much more familiar phenomenon than by heavy particles. Available ionizing heavy particles are by far less abundant than photons but there are several circumstances where they play an essential role. However, there are very few studies on the dynamics of water fragmentation by heavy ions, from both the experimental and theoretical points of view. In case of heavy particles, the collision with water molecules involves collision channels which are not present in the photon or electron cases and whose dynamics are not well described by existing theoretical models, making the experimental data essential to understand and quantify the effects of the ionizing radiation.

This paper has three purposes. The first is to give to the reader a general view of some of the environments where the interaction between heavy ions and water occurs. Thus, in the first sections of this paper, we describe the role played by heavy ions in splliting water in some important scenarios of four branches of sciences: planetary sciences, Precambrian research, cometary atmospheres and tumor therapy. The second is to describe the experimental procedures and results of recent measurements performed by the authors with C^{3+} and O^{5+} ions on water molecules in the vapor phase. These are the first measurements to cover a broad range of fragmentation yields and which have opened the perspective of identifying common signatures of water fragmentation by particles of different types, energies and charge states. Finally, the third is to show that water fragmentation, either by photons, electrons, protons or heavy particles presents universal patterns. This is a key result to organize several apparently dissociated collision regimes allowing a better modeling of the interaction between heavy particles and water.

II. WATER RADIOLYSIS

Before we describe some of the environments where heavy ions act as important ionizing agents of water molecules in general, we briefly describe how these ions can affect their chemical composition by looking at the important case of liquid water. Swift ions passing through liquid water remove electrons from the water molecules leaving a track of ionized species. The final inventory of the new species generated is related to a complex sequence of events which are usually classified as physical, physicochemical and chemical stages. During the first 10^{-15}s from the primary electron removal event, the molecular ion relaxes generating ionic fragments and electrons which can produce further ionizations, giving rise to small regions of high ionization densities commonly known as spurs. Between 10^{-15}s and 10^{-12}s the electrons eventually termalize becoming solvated (e^-_{aq}), the H_2O^+ ions diffuse randomly, the spur expands, and some fast ionic reactions, such as $OH^+ + H_2O \rightarrow H^+ + H_2O_2$ occur. Between 10^{-12}s and 10^{-6}s radicals such as OH, H, O as well as e^-_{aq} species migrate randomly and can react with each other through a variety of reactions such as $OH + OH \rightarrow H_2O_2$, $O + H_2O \rightarrow O_2 + H_2$ resulting, in the end, on the removal of most chemically reactive species [1, 2]. Because, as we will show later, heavy ions can produce a much larger variety of primary fragment ions as compared with photons, electrons or protons, some of the final products can be effectively enhanced, as for example, the production of O_2 [3]. The same sort of enhancement occurs in bombardment of ice, where much larger amounts of charged H, O, H_2, and O_2 species are sputtered by highly ion-

izing ^{252}Cf fission fragments as compared with weakly ionizing 0.85 MeV N^+ ions [4].

III. EUROPA

The Jupiter moon Europa is about 670,000 km from Jupiter, has roughly the size of our moon, is smoothly covered with ice and has a very tenuous oxygen atmosphere. Unlike our Earth, the source of oxygen in Europa's atmosphere is not likely to be biologically produced by plants and bacteria. It comes from the bombardment of the surface by H, O and S ions from the Jupiter magnetosphere which erodes the surface by sputtering, splitting water molecules and producing H_2 and O_2 [5]. The hydrogen escapes from the atmosphere while the oxygen is left behind. A further and interesting consequence of this bombardment is the change of the surface reflectance for UV radiation [6] as observed by the Galileo spacecraft. Water radiolysis can produce, for example H + OH radicals which, after diffusion, can lead to a chemical combination of two OH radicals yielding H_2O_2. Laboratory experiments [6] show that the reflectance of water ice with just 0.16 % of H_2O_2 results in a decrease of 20 % of the surface reflectance at wavelengths of 210 nm as compared with pure water ices. As stressed in Ref. [6], the abundance of H_2O_2 and the existence of O_2 in the atmosphere demonstrate that the surface chemistry on Europa is dominated by water radiolysis induced by energetic heavy particle bombardment.

IV. OKLO NATURAL FISSION REACTOR

In the beginning of 1970s, a uranium shipment to France from a mine near the Oklo river, central-east Gabon, Africa, was found tinily depleted from the usual 0.7202 % ^{235}U fissionable isotope abundance. The reason for this depletion was found to have its origin in the Precambrian period, about 2 billion years ago. By that time, the evolution of plants and algae started the increase of atmospheric oxygen. Uranium has a peculiar chemistry which makes it insoluble in water under oxygen-free conditions but soluble in its oxidized form, UO_2. With the increase of oxygen in the atmosphere as well as in the ground water, the UO_2 began to form and dissolve, becoming present as trace elements in flowing waters. In the Oklo region there are evidences that some quite peculiar microorganism has the ability to collect and concentrate uranium [7]. The U started then to be deposited at higher concentrations at that locations. The differences in the life-time of ^{235}U and ^{238}U is such that, by that time, the fraction of ^{235}U was around 3% and, when an enough amount of U was accumulated by these strange bacteria, a self-sustained chain reaction started, lasting around 1 million years [8, 9]. At critical operation, fission fragments from ^{235}U could directly interact with water, producing further amounts of O_2 as by-products. This extra O_2 not only favored the solubility of fission products but also modified the near-field redox conditions making new oxidized species such as, for example Pb_3O_4. On the other hand, in zones rich in organic matter it could favor the oxygen consumption resulting in a reducing environment [9]. The water radiolysis by heavy ion fission fragments thus plays an important role in the understanding of this natural reactor.

V. COMETARY X-RAYS

The Sun emits a continuous stream of particles whose major constituents are electrons and protons, and minor ones are C, N, O, Ne, Mg, Si, etc. The heavy ions are found in several charge states and their interactions with planetary and cometary atmospheres are responsible for a broad variety of phenomena such as auroras, x-ray emission, atmospheric chemistry, etc. The interaction of highly-charged ions with planetary and cometary gases such as hydrogen, methane and water not only produces ionization and dissociation of these atoms and molecules but also changes the ion charge state through electron capture and stripping. Electron capture in excited states can result in a subsequent decay through emission of photons in the ultra-violet or x-ray regions, which can be the major sources of such photons in very cold atmospheres. In 1996 the observation of x-ray emission from the comet Hyakutake was reported [10]. Being icy bodies, the emission of UV and X-rays from such objects was unexpected. The origin of such emission is presently considered to be a result of charge exchange processes of highly-charged oxygen ions from the solar wind with water [10–12]. For the average velocity of the solar wind ions, the electron capture by O ions occurs into states with high quantum numbers. The captured electron subsequently decays by emitting energetic photons. In addition, the chemical reactions involving the water fragment ions produced by the collisions with the solar wind should be added to those resulting from the photofragmentation process, in order to model the net ionic composition of the ion tail of comets. Due to the lack of information on primary water fragmentation by the solar wind, the magnitude of its effect on the comet ion tail cannot be properly evaluated.

VI. C- ION THERAPY

For about 30 % of cancer patients the disease is well localized within a specific region of the body when it is diagnosed and good chances of cure are obtained through chemotherapy, surgery or radiation therapy. In the latter, the clinical aim of maximizing damage in the tumor sites while minimizing damages to healthy surrounding tissue has lead to the use of protons and, more recently, carbon ions to provide high spatial-specific damage profiles [13–18]. In radiation or particle therapy there is a possibility that the particle interacts directly with critical components of the cell or with water. The latter case is known as indirect action and the damage is made by producing free radicals resulting from the interaction of the bombarding particles with water molecules. These radicals can diffuse and make subsequent damage to the mitochondria, enzymes or DNA. It is estimated that 75 % of the x- ray damage in mammalian cells are due to the action of the OH radical. As these radicals are extremely reactive, the diffusion

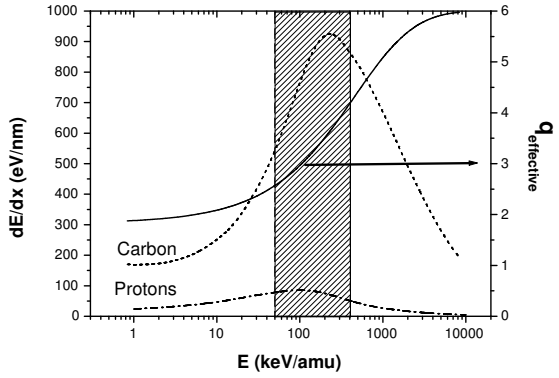

FIG. 1: Energy loss of protons and C-ions in water [19]. The right abscissa gives the C ion effective charge [21], indicated by the dashed curve. The energy region covered by the present measurements is indicated by the dashed area.

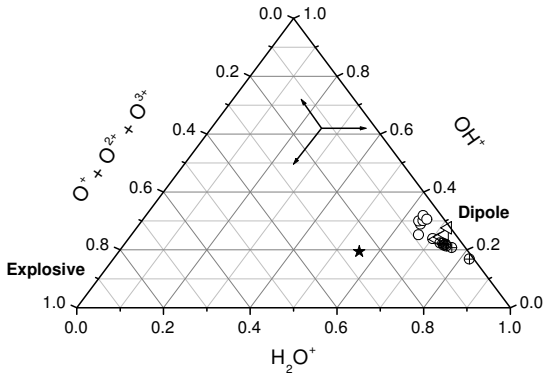

FIG. 2: Ternary plot of probabilities for H_2O^+, OH^+, and $\Sigma_q O^{q+}$ formation by proton ionization (open circles), (Ref. [22]); electron ionization (crossed circles) (Ref. [23]); 6.7 MeV/amu Xe^{44+} ionization (star), Ref. [2]; and photofragmentation results from Ref. [24] (side open triangles). The three diverging arrows in the upper side of the graph indicate how a particular data point is connected with each of the three axes. The different data belonging to the same family of symbols corrrespond to different projectile energies.

length must be within about 20 Å from the target. Recently, good effective radiotoxic responses from C-ion tumor therapy was reported [14–18]. The high ionization densities within the Bragg peak make normal DNA enzymatic repair difficult in contrast to low LET (Linear Energy Transfer) electron, proton and photon irradiation [13]. In spite of C- ion therapy being in current use there are no previous measurements, in the Bragg peak region, of water fragmentation by C ions .

The Bragg peak is where most of the energy of the ionizing particle is deposited and the behavior of several physical systems under the effect of heavy particle irradiation depends on that information. For carbon ions, the energy of the ions at the top of the Bragg peak is nearly 250 KeV/amu [19, 20], with an average charge state of approximately q = 3 [21]. Here, we report the general behavior of the branching ratios for positive ions production in collisions of C^{3+} ions on water molecules at energies around the Bragg peak. The region of the Bragg peak covered in this work is shown in Fig. 1.

VII. PREVIOUS DATA OF ELECTRONS, PHOTONS, PROTONS AND HEAVY IONS

Previous measurements of the absolute yields for fragmentation of water through electron removal - essentially ionization - have been carried out by photons, electrons, protons and Xe^{44} ions. These measurements are displayed in Fig. 2, where the ternary graph shows the normalized fractions of H_2O^+, OH^+ and $\Sigma_q\ O^{q+}$ cross sections by proton ionization of Ref. [22] in the 100 - 400 keV range, electron ionization from Ref. [23] in the 40 - 1000 eV range, 6.7 MeV/amu Xe^{44+} ionization from Ref. [2], and photofragmentation results from Ref. [24] in the 30 - 60 eV range. The sum of the three fractions was made equal to one. It is clear that the photon, electron and proton data tends to cluster with the same $\Sigma_q\ O^{q+}$ and slightly different H_2O^+, OH^+ fragmentation fractions. It is also noteworthy that, for each of these clusters, the fragmentation fractions are quite independent of the particle energy. On the other hand, the 6.7 MeV/amu Xe^{44+} fragmentation fractions are clearly different from the others, with a larger amount of the $\Sigma_q\ O^{q+}$ fractions.

The results for protons, electrons and photons displayed in Fig. 2 clearly show that the fragments follow a sequential distribution with $H_2O^+ > OH^+ > \Sigma_q\ O^{q+}$. This distribution is characteristic of the dipole ionization of the water molecules [24] and express the decay probabilities following the ionization of one of its four valence molecular orbitals $1b_1$, $3a_1$, $1b_2$ and $2a_1$, with ionization energies of 12.6, 14.7, 18.5 and 32.2 eV, respectively [24]. This dipole, sequential fragmentation pattern, has been always assumed to be *the* ionization pattern, independently of the particle type and energy, in water radiolysis modeling [1]. The former particles never reach the explosive regime, when the $\Sigma_q\ O^{q+}$ become the major fragmentation products. In fact, not even the Xe^{44+} data reach the explosive regime, when the above sequence is inverted, and the $\Sigma_q\ O^{q+}$ fraction becomes the major fragmentation product. In the following sections we show that collision channels other than ionization can perform collisions which are hard enough to reach the explosive regime.

VIII. EXPERIMENT

Mono-energetic O^+ and C^+ beams are delivered by the 4MV Van de Graaff accelerator of the Catholic University of Rio de Janeiro. A 90^0 magnet analyzes the primary beam, making its charge/mass and energy selection. Subsequently, the beam passes through a striping gas cell producing a variety of charged daughter beams. The desired charge state compo-

nent is then selected and directed onto the experimental line by a switching magnet. After collimation, the beam is further cleaned from spurious components just before the collision chamber by a third small magnet.

The target cell is placed inside the collision chamber and connected to an effusive water vapor set-up. The set-up is composed by a manifold connecting a needle valve to a Pyrex bottle containing 10 ml of de-ionized water, which is first pumped by an rough pump. When the pressure inside the bottle decreases down to a critical value, the water changes phase into ice. The pump is then valved off and the bottle naturally warm up . The process is repeated several times to drive out any remaining dissolved gas, in order to assure a pure H_2O target. The water is then allowed to sublimate into the cell through a needle valve.

A capacitive manometer (MKS-Baratron) provides an absolute measurement of the pressure inside the gas cell. Determination of the gas pressure for water vapor is more difficult compared to more standard molecular gases. Working with H_2O requires longer times for the system to reach the equilibrium (order of a few minutes) and a significant drift of the zero reading of the manometer can occur. We overcame this difficulty by doing sets of short runs and by checking the zero reading of the gauge each run. Typical working pressures employed during the measurements were kept between 0.5 to 1 mbar, always under single collision conditions.

After interacting with the target, the projectile beam leaves the collision chamber and an analyzing magnet separates the projectile beam from its products. The final projectile charge state will define the collision process related to the molecular ionization/break-up. For example, the O^{5+} projectile can pick up one electron from the H_2O target (electron capture process) leading to a final projectile charge state of O^{4+}. All the beam components are split and detected together by a position sensitive detector placed at the end of the beam line, 4 m downstream. Micro-channel plates detectors usually present a loss of local efficiency due to saturation effects when the number of particles/channel is increased. In this work, as the beam image is very important to separate the different collision channels, it was necessary to work with small counting rates for which the local efficiency was found to be constant. For O^{5+} projectiles, for example, we have found 500 particles/sec as being our upper limit. Therefore, 250 to 350 particle/sec were used throughout the measurements.

The charged target products, H^+, O^{q+}, OH^+ and H_2O^+ resulting from the interaction with the incident projectile beam are collected by a transverse electric field. The use of a strong electric field (960 V/cm) assures the maximum collecting efficiency for all target products. These slow ions pass the electrodes, enter into a field free region, and finally go onto a microchannel plate detector. The target products are separated and analyzed by a standard time-of-flight technique in coincidence with the position-sensitive projectile detector output. The recoil-ion detection efficiencies are obtained using the same procedure described by Santos et al. [25, 26]. In Fig. 3 we have a typical time-of-flight spectrum for 2.0 MeV O^{5+} on H_2O. The H_2O^+ production for the electron capture channel is clearly reduced when compared with the ionization channel.

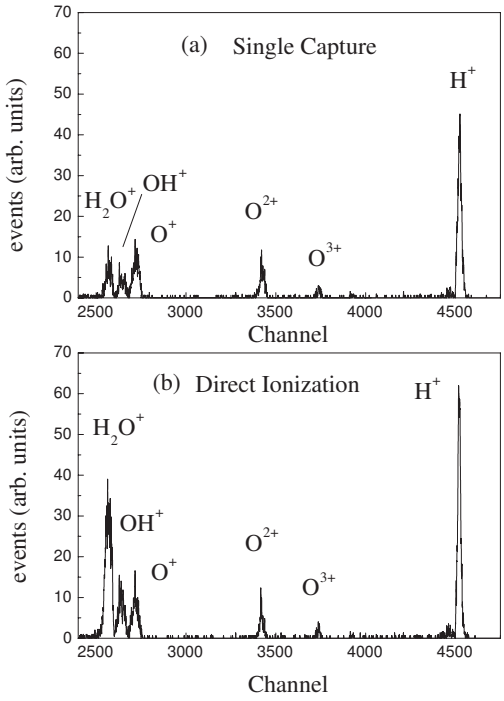

FIG. 3: Time-of-flight spectra for electron capture and direct ionization by 2.0 MeV O^{5+} on water vapor molecules.

IX. EVIDENCE OF EXPLOSIVE FRAGMENTATION

The experiment described above measured the fragmentation of water due to three different collision channels: ionization, electron capture and electron loss. These three channels have different dynamics and energy transfers. For example, for C^{3+} at 3.5 MeV the energy transfer in the ionization channel is $\cong$ 60 eV while for the electron capture channel is $\cong$ 200 eV. These large differences in the energy transfer as well as the much smaller impact parameter in which capture occurs at this energy compared to ionization give rise to large differences in the fragmentation pattern. This is indeed show in Fig. 4, where the present data is added to the data shown in Fig. 2. The possible fragmentation yields are now scattered along a broad range of Σ_q O^{q+}fractions, ranging from the dipole values, around 5 %, to a really explosive dynamics, with the Σ_q O^{q+} fraction lying around 80 %. The data corresponding to the most explosive outcome is associated to processes involving high energy transfers and/or close collisions: high-energy electron capture and low-energy electron loss. As the collision becomes more distant and involving smaller energy transfers, the fragmentation pattern goes towards the dipole characteristics. For example, the most explosive channels and energies shown in Fig. 4 are electron capture (closed triangles) at high velocities and electron loss (closed circles) at low velocities. For electron capture, the collision becomes softer as the velocity decreases and this family of data points moves, along

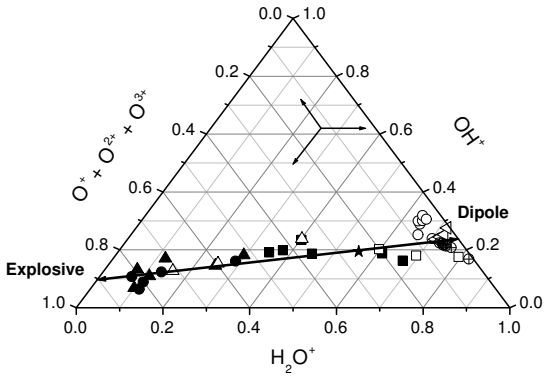

FIG. 4: Same as Fig. 2 including fragment formation by C^{3+} ionization (closed squares), capture (closed triangles) and loss (closed circles), O^{5+} ionization (open squares) and capture (open triangles). The line is a fit through the data. For the C and O data shown, the energy increases along this line from right to left for the ionization and capture channels and from left to right for the loss. The explosive regime is reached for high energy electron capture and low energy electron loss.

the indicated line, from the explosive region (higher velocities) towards the dipole region (lower velocities) of the graph. For electron loss the reverse behavior occurs.

The coalescence of the data on the line shown in Fig. 4 is also remarkable. This coalescence is pretty much insensitive to the collision energy, collision channel, particle type and charge state. It can be shown that this coalescence is a related to the constraint that all fragment products are due to either one- or two-electron removal cross sections plus a decay scheme which is independent of the collision dynamics [27]. This last point is an indication that the removal and the decay processes can be well separated in time.

X. CONSEQUENCES OF EXPLOSIVE PRIMARY FRAGMENTATION

From Fig. 4 it is clear that the O^{q+} production by heavy ions for energies around the Bragg peak is much larger than the mere 5% production by electrons, photons and protons at any energy. This finding can explain the observed increase of O_2 by high LET particles. After being produced by the primary collision, the O ion rapidly neutralizes through electron transfer. The resulting oxygen can be either in the $O(^1D)$ or in the $O(^3P)$ states. The singlet $O(^1D)$ reacts rapidly with water through the reactions $O + H_2O \rightarrow H_2O_2$ or $O + H_2O \rightarrow 2OH$ [2, 28]. On the other hand, the ground state $O(^3P)$ is reasonably inert in water and can survive enough time to eventually react with OH through the reaction $O(^3P) + OH \rightarrow HO_2$, producing HO_2. The suggestion of Ref. [3] that the increase of O_2 production by high-LET particles is due to an increase of primary O production is supported by our findings and is a consequence of the increasing importance of the double electron removal at the Bragg peak region [27].

XI. CONCLUSIONS

Here we find evidence that in C and O ions interaction with water, a large fraction of molecules completely blows out producing large abundances of H^+ and O^+ fragments in comparison to proton, electron and photon irradiation, or even heavy ions with energies outside the Bragg peak region. Indeed, the cross sections for O^+ production by C^{3+} ions at the Bragg peak are about one order of magnitude larger as compared with those for the above mentioned projectiles at any energy [23, 24, 27]. Our findings have straightforward implications in the subsequent fast chemistry at the ionization site, such as the production of the highly reactive OH radicals, hydrogen peroxide, H_2O_2, as well as O_2, showing that the marked differences in primary O production between high-LET particles and low-LET electrons, protons and photons can be the possible source of the observed differences in the final products of ionizing particles.

Acknowledgments

The authors wish to thank Drs. G. M. Sigaud and M. B. Shah for fruitful discussions and review of the manuscript. This work was supported in part by the Brazilian agencies CNPq, CAPES, FAPERJ, and MCT (PRONEX).

[1] J. A. LaVerne, Rad. Res. **153**, 487 (2000).
[2] G. H. Olivera, C. Caraby, P. Jardin, A. Cassimi, L. Adoui, and B. Gervais, Phys. Med. Biol. **43**, 2347 (1998).
[3] C. Ferradini and J. P. Jay-Gerin, Rad. Phys. Chem. **51**, 263 (1998).
[4] V. M. Collado, L. S. Farenzena, C. R. Ponciano, E. F. da Silveira, and K. Wien, Surf. Sci. **569**, 149 (2004).
[5] J. F. Copper, R. E. Johnson, B. H. Mauk, H. B. Garret, and N. Gehrels, Icarus **149**, 133 (2001).
[6] R. W. Carlson et al., Science **283**, 2062 (1999).
[7] Nick Lane, *Oxigen*, Oxford University Press: New York, 2002.
[8] D. J. Mossman, F. Gauthier-Lafaye, and S. E. Jackson, Precambrian Research **106**, 135 (2001).
[9] V. Savary and M. Pagel, Geoch. and Cosmoch. Acta **61**, 4479 (1997).
[10] C. M. Lisse et al., Science **274**, 205 (1996).
[11] C. M. Lisse et al., Science **292**, 1343 (2001).
[12] T. E. Cravens, Science **296**, 1042 (2002).
[13] A. Brahme, Int. J. Rad. Oncol. Biol. Phys. **58**, 603 (2004).
[14] Y. Iwadate, J. E. Mizoe, Y. Osaka, A. Yamamura, and H. Tsujii, Int. J. Rad. Oncol. Biol. Phys. **50**, 803 (2001).
[15] T. Miyamoto, N. Yamamoto, H. Nishimura, M. Koto, H. Tsu-

jii, J. Mizoe, T. Kamada, H. Kato, S. Yamada, S. Morita, K. Yoshikawa, S. Kandatsu, and T. Fujisawa, Radioth. and Oncol. **66**, 127 (2003).
[16] N. Yamamoto, T. Miyamoto, H. Nishimura, M. Koto, H. Tsujii, H. Ohwada, and T. Fujisawa, Lung Cancer **42**, 87 (2003).
[17] K. Akakura , H. Tsujii, S. Morita, H. Tsuji, T. Yagishita, S. Isaka, H. Ito, H. Akaza, M. Hata, M. Fujime, M. Harada, amd J. Shimazaki, Prostate. **58**, 252 (2004).
[18] D. Schulz-Ertner, A. Nikoghosyan, C. Thilmann, T. Haberer, O. Jkel, C. Karger, G. Kraft, M. Wannenmacher, and J. Debus, Int. J. Rad. Oncol. Biol. Phys. **58**, 631 (2004).
[19] J. F. Ziegler, J. P. Biersack, and U. Littmark, *The Stopping and Range of Ions in Solids*, Pergamon: New York, 1985.
[20] P. L. Grande and G. Schiwietz, in *Advances in Quantum Chemistry*, **45**, 7, Elsevier: Berlin, 2004; CASP 3.1 sofware http://www.hmi.de/people/schiwietz/casp.html
[21] E. C. Montenegro, S. A. Cruz, and C. Vargas-Aburto, Phys. Lett. **92A**, 195 (1982).
[22] U. Werner, K. Beckord, J. Becker, and H.O. Lutz, Phys. Rev. Lett. **74**, 1962 (1995).
[23] M. V. V. Rao, I. Iga, and S. K. Srivastava, J. Geophys. Res. **100**, 26421 (1995).
[24] K. H. Tan, C. E. Brion, Ph. E. Van der Leeuw, and M. J. Van der Wiel, Chem. Phys. **29**, 299 (1978).
[25] A.C.F. Santos, W.S. Melo, M.M. Sant'Anna, G.M. Sigaud, and E.C. Montenegro, Phys. Rev. A **63**, 062717-1, (2001).
[26] A.C.F. Santos, W.S. Melo, M.M. Sant'Anna, G.M. Sigaud, and E.C. Montenegro, Rev. Sci. Instrum. **73**, 2396 (2002).
[27] H. Luna and E. C. Montenegro, Phys. Rev. Lett. **94**, 043201 (2005).
[28] J. Meesungnoen, A. Filali-Mouhim, N. S. Ayudhya, S. Mankhetkorn, and J. P Jay-Gerin, Chem. Phys. Lett. **377**, 419 (2003).